

Photoswitchable layer-by-layer coatings based on photochromic polynorbornenes bearing spiropyran side groups

Paula P. Campos^{1,2}, Aishling Dunne¹, Colm Delaney¹, Cara Moloney¹ †, Simon E. Moulton³, Fernando Benito-Lopez⁴, Marystela Ferreira⁵, Dermot Diamond¹ and Larisa Florea^{1}*

¹ Insight Centre for Data Analytics, National Centre for Sensor Research, School of Chemical Sciences, Dublin City University, Dublin, Ireland

² Post-Graduation Program in Materials Science and Technology (POSMAT), Estate University of São Paulo (UNESP), Brazil

³ ARC Centre of Excellence for Electromaterials Science, Faculty of Science, Engineering and Technology, Iverson Health Innovation Research Institute, Swinburne University of Technology, VIC 3122, Australia

⁴ Microsystems & Materials for Lab-on-a-Chip (AMMa-LOAC) Group, Microfluidics Cluster UPV/EHU, Analytical Chemistry Department, University of the Basque Country

⁵ Federal University of São Carlos-Sorocaba (UFSCAR), Brazil

†Current address: School of Chemistry, University College Dublin, Belfield, Dublin 4, Ireland

KEYWORDS: Layer-by-Layer, Spiropyran, Photo-responsive, Photochromic, Coatings.

ABSTRACT

Herein, we present the synthesis of linear photochromic norbornene polymers bearing spiropyran side groups (poly(SP-R)), and their assembly into LbL films on glass substrates when converted to the poly(MC-R) under UV irradiation. The LbL films were composed of bilayers of poly(allylamine hydrochloride) (PAH) and poly(MC-R), forming (PAH/poly(MC-R))_n coatings. The MC form presents a significant absorption band in the visible spectral region which allowed the LbL deposition process to be tracked by UV-Vis spectroscopy, showing a linear increase of the characteristic MC absorbance band with increased number of bilayers. The thickness and morphology of the (PAH/poly(MC-R))_n films were characterised by ellipsometry and Scanning Electron Microscopy, showing a height of ~27.5 nm for the first bilayer and an overall height of ~165 nm for the (PAH/poly(MC-R))₅ multilayer film. Prolonged white light irradiation (22h) showed a gradual decrease of the MC band by 90.4 ± 2.9% relative to the baseline, indicating the potential application of these films as coatings for photo-controlled delivery systems.

INTRODUCTION

A great number of stimuli-responsive materials, mostly involving polymers, have been reported in the recent years, with applications spanning optoelectronics,¹ surface coatings,² photonics,³ biomedicine⁴ and drug delivery.⁵ Photo-responsive materials constitute a subset of particular interest, as the stimulus can be applied remotely, in a non-invasive manner. Photo-responsive materials have been the subject of many investigations over the past decade due to their numerous potential applications, including optical memory devices,⁶ switches and displays,⁷ artificial muscles,⁸ soft-actuators⁹ and drug delivery.¹⁰ Such materials are characterised by their ability to

absorb light energy of particular wavelengths, resulting in intra- or inter-molecular transformations. These changes in molecular structure and configuration are typically accompanied by changes in the optical properties,¹¹ molecular charge,¹² and dipole moment.¹³

In the field of photo-responsive polymers, the Layer-by-Layer (LbL) approach offers a simple and effective method to fabricate uniform thin films which are capable of photo-modulation. The LbL technique is based on electrostatic interactions between oppositely charged materials and can be achieved by various methods, such as dip-coating, spin-coating, spray-coating and flow based techniques.¹⁴⁻¹⁶ In LbL dip-coating, a substrate is alternately immersed in solutions containing positively (polycations) and negatively (polyanions) charged species, which adsorb to the surface of the substrate. If these electrostatic interactions can be disturbed externally by photo-irradiation, then triggered disassembly of the layers can be realised.¹⁷

In this context, we have focussed our investigations on the synthesis of LbL coatings based on photochromic norbornene polymers bearing spiropyran side groups, which are capable of disassembling upon photo-stimulation. The photochromism of spiropyran (SP) is caused by photo-cleavage of the C_{spiro}-O bond upon irradiation with UV light.¹⁸ This cleavage generates a conformational rearrangement between the uncharged SP and ring-opened charged zwitterionic merocyanine (MC) forms. The latter possesses a significant absorption band in the visible spectral region which enables tracking of the switching process via UV-Vis spectroscopy. As exposure of the MC form to visible light induces reversion to its closed uncharged SP form, it is therefore possible to modulate the charge of this species simply by irradiation with light (UV and Vis).

When utilised for building polyelectrolytes multilayers, MC-functionalised polymers appear to play the role of the anionic polyelectrolyte due to the anionic nitrophenolate group of MC which is largely localised on the oxygen atom, in contrast to the positive charge of the indoline nitrogen,

which is extensively delocalised over the indoline ring.¹⁹ Electronic structure calculations of the closed spiropyran (SP)/ open merocyanine (MC) isomers support this interpretation of experimentally observed behaviour of MC-functionalised polymers, indicating that the phenolic oxygen anion site in MC is present at a much higher charge density than the indoline nitrogen cation site²⁰. SP functionalised polymers have been reported in LbL films in several studies. Li *et al.* encapsulated SP units in block copolymers based on poly(*tert*-butyl acrylate-*co*-ethyl acrylate-*co*-methacrylic acid (PTBEM) to produce negatively charged SP-PTBEM micelles which were then intercalated with positively charged MgAl-layered double hydroxide (LDH) nanoplatelets.²¹ This (SP-PTBEM/LDH)_n organic–inorganic ultrathin film displayed fast SP-MC transformation under UV/visible light irradiation cycles with enhanced reversibility and photostability, compared to SP-PTBEM solution or pristine SP-PTBEM films obtained by a drop-casting method.²¹ In a different approach, Pennakalathil *et al.*, developed a LbL film composed of negatively charged poly(acrylate, merocyanine) (PMC) and positively charged poly(diallyldimethylammonium chloride) (PDADMAC). This (PMC/PDADMAC)_n (n=1-5) served as a sacrificial layer, on which a second LbL film (sample layer) composed of negatively charged poly(sodium 4-styrenesulfonate) (PSS) and PDADMAC, (PDADMAC/PSS)_n (n=25, 50, 75) was deposited. Under white light irradiation in water, conversion of MC to the neutral SP form was induced, causing the disassembly of the sacrificial layer and release of the sample layer.¹⁹

Herein we report the synthesis and characterisation of linear photochromic polynorbornenes bearing spiropyran (poly(SP-R)) side groups. After irradiation with UV light (poly(MC-R)), these polymers were used as anionic polyelectrolytes and intercalated with poly(allylamine hydrochloride) (PAH), enabling LbL coating to be successfully achieved on glass slides. Successive deposition of the (PAH/poly(MC-R)) bilayers was confirmed by UV-Vis spectroscopy.

The thickness, roughness and morphology of the coating was characterised by ellipsometry and Scanning Electron Microscopy (SEM), respectively. Photo-induced disassembly of the layers upon white light irradiation was also demonstrated.

MATERIALS AND METHODS

Reagents. 5-norbornene-2-carboxylic acid, *exo*- (Sigma-Aldrich), 1-(2-hydroxyethyl)-3,3-dimethylindolino-6'-nitrobenzopyrlospiran (SP1) (TCI Europe), *N,N'*-dicyclohexylcarbodiimide (DCC) (Sigma-Aldrich), 4-(dimethylamino)pyridine (DMAP) (Sigma-Aldrich) and Grubbs generation-II catalyst (Sigma-Aldrich) were used as received. For the SP-R and poly(SP-R) synthesis, dry tetrahydrofuran and dry dichloromethane solvents were purchased from Sigma-Aldrich and used as received. For the UV-Vis characterisation and LbL procedure, dimethylformamide (DMF) was purchased from Sigma-Aldrich and used as received. Microscope cover glasses (24 x 60 mm, thickness = 0.085 to 0.115 mm, cut in 7 x 50 mm rectangles) were purchased from Marienfeld Superior, Germany. Poly(allylamine hydrochloride) (PAH, $M_w = 15000$) was purchased from Sigma and supplied by Dr. Simon Moulton, UOW.

Instrumentation. ^1H NMR spectra of the poly(SP-R)) were performed in CDCl_3 on a Bruker Avance® spectrometer (400 MHz.). The particle size of poly(SP-R)) and their surface charge (ζ -potential) was estimated from dynamic light scattering (DLS) using a Malvern Zetasizer Nano ZS (Malvern Instruments, Ltd, United Kingdom). UV-Vis analysis of the SP-R, poly(SP-R) solutions, poly(SP-R) LbL coatings on glass slides and the disassembly assay were performed on a Cary 50 spectrophotometer (Varian). Morphological studies of LbL coatings on silicon substrates were performed using scanning electron microscopy (SEM) on a Carl Zeiss EVOLS 15 system at an accelerating voltage of 9.64 kV. Prior to SEM imaging, the silicon substrates were coated with 10

nm of gold. The thickness of films was measured by profilometry using a Dektak 150 Surface Profiler from Veeco Instruments Inc. Photo-conversion of monomer (SP-R to MC-R) and polymer (poly(SP-R) to poly(MC-R)) solutions and LbL films ((PAH/poly(SP-R))_n to (PAH/poly(MC-R))_n) was achieved using a UV chamber (CL-1000 Ultraviolet Crosslinker UVP). The reverse process was performed using white light irradiation provided via a Fiber Lite LMI-6000 obtained from Dolan-Jenner Industries. The maximum light output of the lamp is 780 Lumens, and the intensity control of the light output was fixed at 100%. In all cases the sample was placed 3 cm away from the light source.

Synthesis of the monomer, namely *exo*-5-norbornene-2-carboxylic acid spiropyran ethyl ester (SP-R). The monomer (SP-R) was prepared from the reaction of *exo*-5-norbornyl carboxylic acid with SP1 in the presence of DCC and DMAP as described elsewhere.^{22,23}

Synthesis of poly(5-norbornene-2-carboxylic acid spiropyran ethyl ester) (poly(SP-R)). Ring-opening metathesis polymerisation (ROMP) was performed using a modified version of the previously described method.²³ Briefly, in a typical procedure, a solution of the monomer SP-R in rigorously degassed CH₂Cl₂ was poured into a CH₂Cl₂ solution of Grubbs catalyst second generation, to obtain a final molar ratio SP-R: catalyst of 300:1 (poly(SP-R)₃₀₀). The final monomer concentrations were all 10 mM. The polymerization was left to stir at room temperature for 14h. To stop the polymerization, excess ethyl vinyl ether was added under stirring and the solution was exposed to the atmosphere for 30 min (Figure 1). The polymers were precipitated by pouring the reaction solutions into hexane and collecting the precipitate using vacuum filtration.

poly(SP-R): Yield: 67% (white powder). ¹H NMR (400 MHz, CDCl₃): δ 7.89 (br s, 2H, spiro^{5,7}), δ 7.15-6.90 (br d, 2H, spiro^{4,8}), δ 6.78 (br s, 2H, spiro^{5,6}), δ 6.59 (br s, 2H, spiro^{7,4}), δ 5.77 (br s, 1H, spiro³), δ 4.95-5.4 (br d, 2H, CH of double bonds in polymer backbone), δ 4.09 (br s, 2H, O-

CH₂), δ 3.3-3.4 (br d, 2H, -N-CH₂), δ 2.8-2.9 (br d, 2H, cp^{1,5}), δ 2.6 (br s, 1H, cp³), δ 2.3 (br s, 1H, cp²), δ 2.0-1.5 (br m, cp^{2,4}, -CH₃).

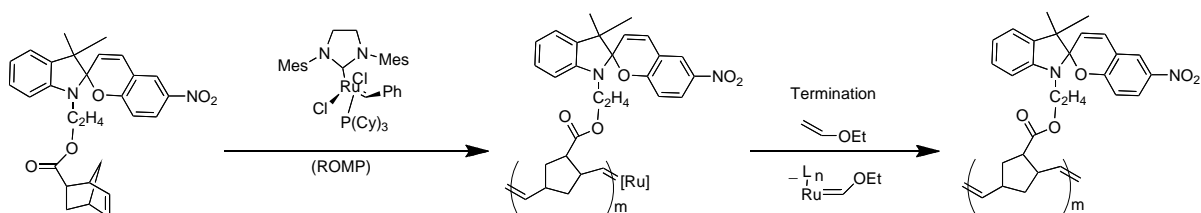


Figure 1. Scheme showing the polymerization of *exo*-5-norbornene-2-carboxylic acid spiropyran ethyl ester (SP-R) by ring-opening metathesis polymerization and the termination of the reaction.

Layer-by-layer deposition. Layer-by-layer deposition of polymers was performed on glass and silicon substrates. The glass slides were firstly cleaned with different solvents: DI water, acetone and ethanol. Following this, the glass slides were immersed in a NH₄OH/H₂O₂/H₂O (1:1:5, V:V:V) solution (75 °C for 10 min), washed with DI water for 1 min, subsequently immersed in a HCl/H₂O₂/H₂O (1:1:6, V:V:V) hydrophilization solution (75 °C for 10 min), and finally washed in DI water²⁴. These treatments generate negative charges on the glass surface due to partial hydrolysis.²⁵ The silicon substrates were cleaned with chloroform and acetone, followed by sonication for 30 min in isopropyl alcohol. The LbL assembly was carried out by a cyclic repetition of the following operations: the substrates were (1) immersed in a PAH solution (1 mg mL⁻¹, pH = 7, adjusted with NaOH solution) for 3 min; (2) washed with DI water for 30 s; (3) immersed in a poly(MC-R) solution (1 mg mL⁻¹ in DMF/H₂O 3/1 (V/V)) for 5 min (the poly(SP-R) solution was previously irradiated with UV light for 3 min to produce poly(MC-R)); (4) washed with DI water for 30 s. The scheme of deposition can be visualized in Figure S1. This sequence (1 to 4) was repeated until the desired number of (PAH/poly(MC))_n bilayers was reached. It should be noted that, as the poly(MC-R) solution retained its purple colour after the first coating, it was not

necessary to irradiate it again with UV light. This is most likely due to the increased polarity of the solution and high concentration of the polymer, resulting in slow kinetics for the reverse closing process to the colourless SP-R form. Deposition of material at each step was monitored using UV-Vis spectroscopy on a Cary 50 spectrophotometer (Varian). For SEM analysis, a (PAH/poly(MC))₅ LbL film on a silicon substrate was achieved by immersing the substrate in decreasing volumes of solution for each bilayer for the purpose of obtaining a film with a step architecture, where each step represents a different number (1 to 5) of bilayers.

Disassembly assay. Glass slides and silicon substrates coated with (PAH/poly(MC))₅ were immersed in a cuvette containing DMF:water (3:1) (V:V) and exposed to prolonged white light irradiation using the Fiber Lite LMI-6000 white light source, at room temperature. The absorbance of the film was measured by UV-Vis spectroscopy every 30 min/60 min. A single exponential model (eq. 1) was used to determine the photo-disassembly constant for the (PAH/poly(MC-R))₅ LbL sample.

$$y = a * e^{-kt} + b \quad (\text{eq. 1})$$

where y is the absorbance at 345 nm, a is the scaling factor, k is the first order photo-disassembly rate constant (min^{-1}), b is the baseline offset, and t is time (min).

The half-life ($t_{\frac{1}{2}}$) for the photo-disassembly was calculated using eq. 2.

$$t_{\frac{1}{2}} = \frac{\ln(2)}{k} \quad (\text{eq. 2})$$

The (PAH/poly(MC-R))_n LbL samples were also analysed by SEM and profilometry.

RESULTS AND DISCUSSION

Synthesis and characterisation of polymers poly(SP-R). Confirmation of polymerization was determined by ¹H NMR, based on the shift of the norbornene olefinic peaks, observed between

6.14 and 6.06 ppm for the monomer to 5.21 and 5.15 ppm for the polymer (poly(SP-R)₃₀₀), as shown in Figure S2. This is due to the opening of the norbornene ring through ring opening metathesis polymerisation. A Poly(SP-R) solution was analysed by DLS in DMF (0.1 mg mL⁻¹) to obtain information about the particle size of poly(SP-R) polymer and its zeta potential (ζ) in both spiropyran and merocyanine states. The values found for the polymer particle size were centred around 206.7 nm, with a polydispersion index (PDI) of 0.43 (Figure S3). UV irradiation of the solution to achieve switching from poly(SP-R) to poly(MC-R), showed two peaks for the zeta potential (ζ), a positive one centred at 95 mV with 22929.7 counts and a negative one centred at -9.87 mV with 127701 counts, due to the zwitterion nature of the merocyanine isomer (Figure S4). Approximately 10 min after the UV irradiation was stopped, the negative peak disappeared almost completely and only a small (2304 counts) positive peak centred at 39.6 mV remains, indicating the structural change accompanying conversion of the MC-R zwitterion to the neutral SP-R in an intermediary form in which the positive charge is steadily decreasing. These results indicate that poly(MC-R) polymers could serve as poly(anions) in LbL coatings (the negative ζ peak considerably larger compared to the positive peak), and that the charge can be cancelled through exposure to white light.

UV-Vis absorption spectroscopy of monomer and polymer solutions. To study the photochromic properties of SP-R and poly(SP-R), solutions of the monomer (0.17 mg mL⁻¹) and polymer (0.17 mg mL⁻¹) were prepared in DMF:water (3:1) (V:V) and analysed by UV-Vis spectroscopy. Reversible photo-induced isomerization was observed for the solutions studied when irradiated with UV (365 nm) and white light (WL), respectively, during 1, 2 and 3 min irradiation cycles (Figure 2). Both solutions showed the typical UV absorbance band centred at λ_{\max} =352 nm and the visible absorbance band (centred at λ_{\max} =550 nm in the case of MC-R

solution and 565 nm for the poly(MC-R) solution) assigned to the π - π^* electronic excitation of the benzopyran part of the molecule and the conjugated merocyanine form, respectively.²⁶ MC isomers are well known for their solvatochromic properties, where their absorbance band is strongly dependent of the polarity of the solvent and the local environment.^{23,27–29} The absorption spectra of the spiropyran monomer and polymer (Figure 1), in both the closed (SP-R, poly(SP-R)) and open (MC-R, poly(MC-R)) forms were similar (Figure 2), which illustrated that the polymerisation of the spiropyran monomer did not have a significant effect on the ground-state properties of the isomers. Moreover, as the UV-Vis spectra of poly(SP-R) solution (Fig. 2B) does not change beyond 2 min of UV irradiation (spectra obtained after 2 min UV is identical with the spectra obtained after 3 min UV) it indicates that equilibrium SP to MC conversion of poly(SP-R) in DMF:water (3:1) is achieved within this time interval. This is in accordance with previous results reported for spiropyran functionalised polynorbornene brushes obtained through surface-initiated ROMP, where the rate constants for the ring-opening equilibrium were calculated to be between 1.04 and $2.84 \times 10^{-2} \text{ s}^{-1}$.²⁷

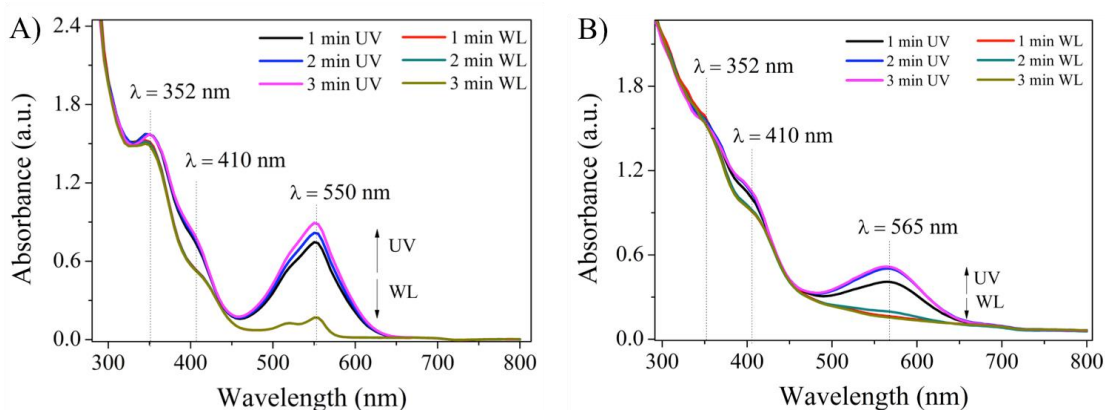


Figure 2. UV-Vis spectra of 0.17 mg mL^{-1} solutions of (A) SP-R monomer and (B) poly(SP-R) in DMF: water (3:1), after 1, 2 and 3 min irradiation with UV and white light (WL), respectively.

The spectra for SP-R monomer and poly(SP-R) solutions after WL irradiation are identical and therefore overlapping, indicating that 1 min of WL irradiation is sufficient in these conditions (solvent and SP-R/poly(SP-R) concentration) to achieve equilibrium MC to SP conversion for both the monomer (A) and polymer (B) solutions, respectively.

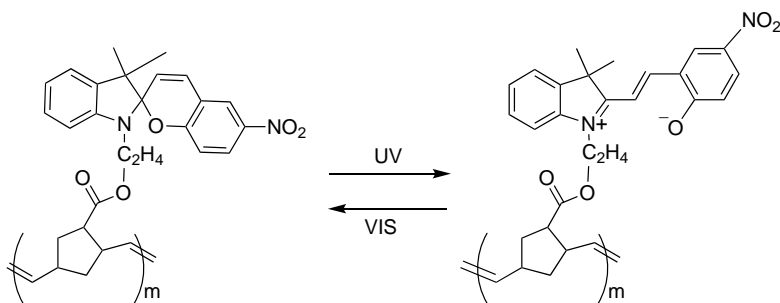


Figure 3. Light-induced reversible switching between the closed spiropyran form (SP) and the open merocyanine form (MC) inside the poly(SP-R) matrix.

UV-Vis absorption spectroscopy of LbL coatings. UV-Vis spectroscopy was employed to monitor the LbL deposition of PAH and poly(MC-R) on glass slides by means of dip-coating, as described in the experimental section (Figure 4). The regular deposition of (PAH/poly(MC-R))₁₀ bilayers was confirmed by a plot of the characteristic absorption band of poly(MC-R) at 345 nm and 590 nm, *versus* the bilayer number (Figure 4C and 4D). This linear increase confirms that the same amount of material is deposited in each step.^{30,31} In the UV-Vis spectra of the film, the main bands of poly(MC-R) at 345 nm and 590 nm are present, as in the solution spectra. However, for the film, the bands are considerably broader, most likely due to aggregation of the material onto the surface, a typical behaviour of layer-by-layer films of this nature.³²⁻³⁴ A representative (PAH/poly(MC-R))₁₀ film on a glass substrate is shown in Figure 4B, as it appears after 3 min of UV irradiation.

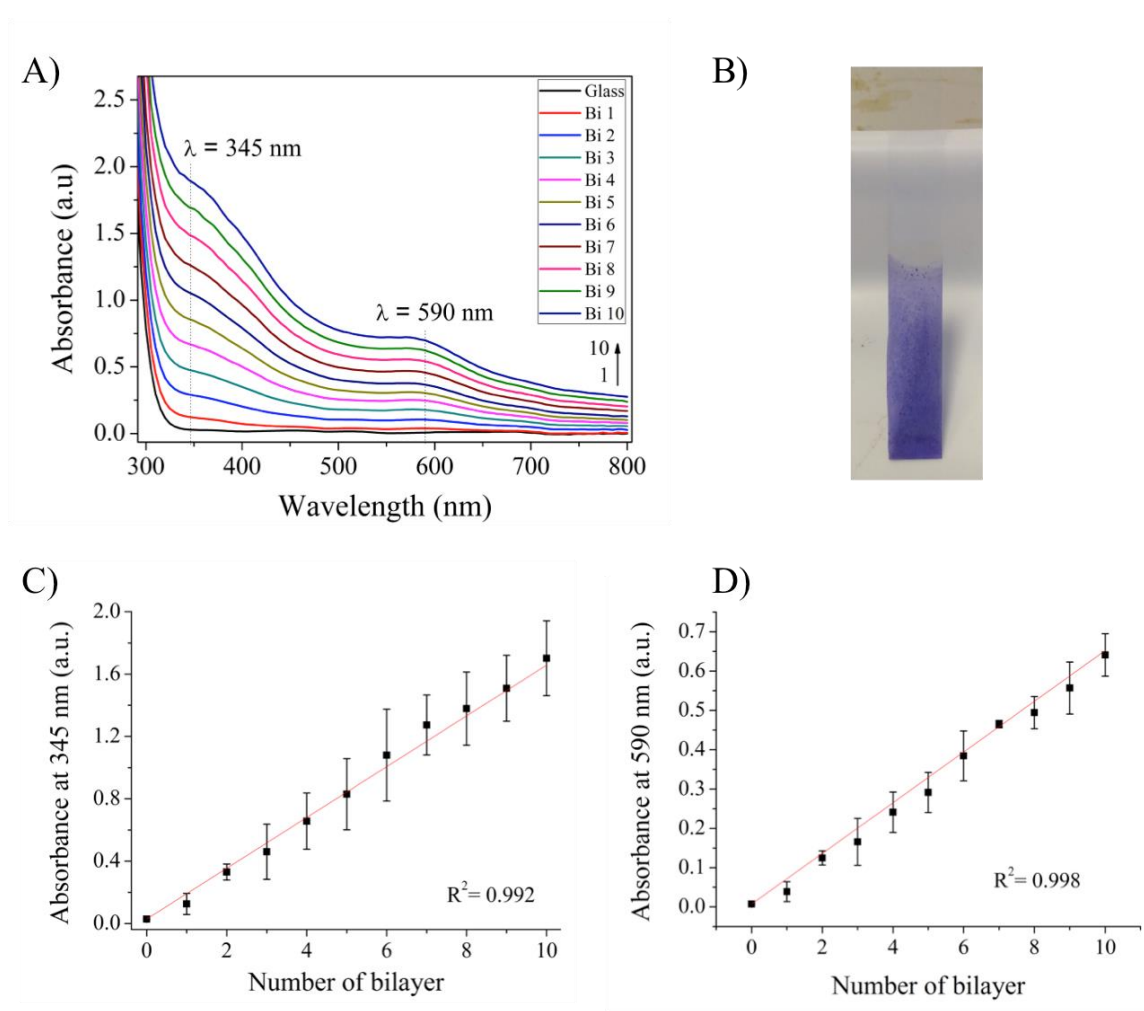


Figure 4. UV-Vis characterisation of PAH/poly(MC-R) bilayers. (A) UV-Vis spectra of each bilayer of the (PAH/poly(MC))₁₀ film; (B) Image of the corresponding (PAH/poly(MC))₁₀ coated glass slide. Plot of the absorbance at 345 nm (C) and 590 nm (D) of (poly(MC-R))_n vs the bilayer number. The film was composed of 10 bilayers. The coating was done on three different glass substrates. The error bars represent the standard deviation of the absorbance at 345 nm (C) and 590 nm (D), respectively, for each bilayer. Error bars represent standard deviations for 3 repeated LbL assemblies.

LbL photo-response. The photochromic behaviour of the LbL coatings was characterised after immobilisation on glass substrates. (PAH/poly(MC))₅ coated glass slides were placed in a cuvette

with DMF:water (3:1) (V:V), subjected to the same UV and white light irradiation cycles as per poly(SP-R) solution (Figure 2B) and analysed by UV-Vis spectroscopy (inside the cuvette). As shown in Figure 5A, the (PAH/poly(MC))₅ LbL film maintains its reversible photochromic behaviour even after immobilisation. UV and white light (WL) irradiation cycles cause an increase (UV) and subsequent decrease (WL) of the merocyanine band. Irradiation of the coated glass slide with UV light for 1, 2 and 3 min, caused an increase of the 590 nm absorbance to 0.05±0.007 a.u., 0.095±0.008 a.u. and 0.125±0.007 a.u. (average and standard deviation, n=3), respectively. Similar to solution studies, irradiation of the LbL film with white light for 1, 2 and 3 min, respectively, caused the disappearance of the 590 nm absorption band. The magnitude of the absorbance change upon UV/white light irradiation cycles in the film (Fig. 5A) is considerably smaller compared to solution (Fig. 2B). This is expected due to the decreased degree of freedom of the SP/MC unit in the immobilised layer. The change in the absorbance at 590 nm between (PAH/poly(SP))₅ and (PAH/poly(MC))₅ after each UV/WL cycle (1, 2 and 3 min, respectively) is shown in Figure 5B.

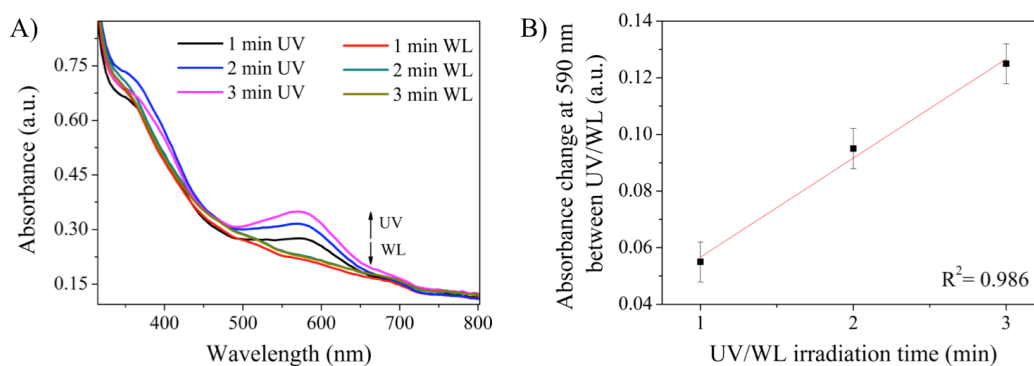


Figure 5. (A) UV-Vis spectra of a 5-bilayer LbL coated glass slide showing the change of the characteristic poly(MC-R) band ($\lambda_{max}=590$) upon three successive UV/white light (WL) irradiation cycles of increased duration (1, 2 and 3 min, respectively); (B) The change in the

absorbance at 590 nm between (PAH/poly(SP))₅ and (PAH/poly(MC))₅ after each UV/WL cycle (1, 2 and 3 min, respectively). The test was done for 3 different glass substrates coated. The error bars represent the standard deviation of the absorbance at UV/WL irradiation cycles, (n=4).

Surface morphology, thickness, and roughness of PAH/poly(MC) multilayers. Scanning Electron Microscopy was used to study the morphology of the layers and the distribution of the material on the substrate. For this purpose, a (PAH/poly(MC))₅ experiments were performed with the aim of creating the LbL step architecture proposed in Figure 6A on the silicon substrate as described in the experimental section. Representative images obtained for the bilayers obtained are shown in Figure 6B, Bi1-5. SEM analysis revealed that from bilayer 3 onwards, complete coverage of the silicon substrate was obtained. In contrast, for the first bilayer, the polymer deposition was not completely homogeneous. This could be attributed to weak interactions between the substrate and low charge-density polymers, resulting in a reduced number of attachment points. Conversely, polymers which exhibit a high charge density offer more attachment points to the substrate surface, thereby resulting more uniformly flat LbL layers.³⁵ The increase in roughness and aggregate formation from 1 bilayer to 5 bilayers is noticeable in the images presented in Figure 6. This is a common observation in LbL studies.^{32,36-38} Profilometer analysis of the (PAH/poly(MC))₅ film gave an estimated total thickness of ~165 nm for the 5-bilayer film (Figure S5), and a thickness of ~27.5 nm for the first bilayer alone (Figure 6-Bi1, Figure S6). This thickness is comparable to other polymeric LbL films³⁹. Profilometry analysis was also performed after the film (PAH/poly(MC))₅ was subjected to photo-induced disassembly. It showed that the thickness of the coating decreased from ~165 nm to ~11 nm, evidencing the release of material from the substrate (Figure S7). Figure S5 reveals sharp peaks around 500 and 600 nm that are not present in Figure S6 (first bilayer). This is in agreement with the aggregates

visualized in the SEM images, which become more obvious with an increased number of bilayers (Bi 1 to Bi 5, Figure 6B). Despite the roughness of the LbL films there is no apparent adverse effect on their photo-response behaviour (Figure 5).

Profilometry analysis of the 5 bilayer film (Figure S5) also reveals sharp peaks around 500 and 600 nm, in agreement with the aggregates visualized on the SEM images (Figure 6). Despite the roughness of the LbL films there is no apparent adverse effect on their photo-response behaviour (Figure 5).

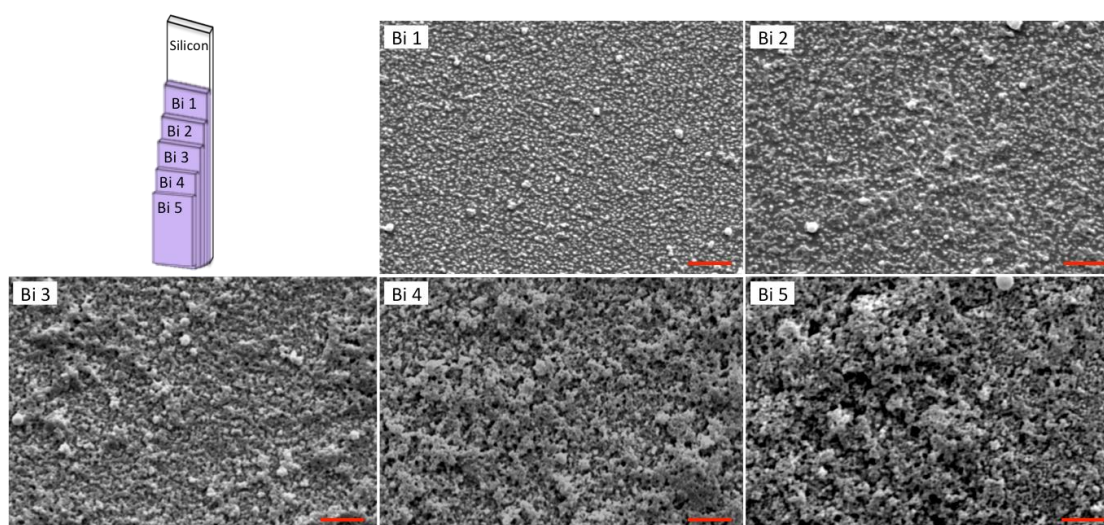


Figure 6. (A) Representative scheme of the $(\text{PAH}/\text{poly}(\text{MC}))_5$ LbL film showing the proposed step architecture and (B) scanning electron microscopy images of each of the steps: $(\text{PAH}/\text{poly}(\text{MC}))_1$ (Bi 1), $(\text{PAH}/\text{poly}(\text{MC}))_2$ (Bi 2), $(\text{PAH}/\text{poly}(\text{MC}))_3$ (Bi 3), $(\text{PAH}/\text{poly}(\text{MC}))_4$ (Bi 4), and $(\text{PAH}/\text{poly}(\text{MC}))_5$ (Bi 5), respectively. Scale bar (red) represents 2 μm .

Photo-induced Disassembly. In order to study the disassembly of the layers by photo-irradiation, the $(\text{PAH}/\text{poly}(\text{MC-R}))_5$ LbL coated glass slide was subjected to white light irradiation. It was expected that by switching the charged poly(MC-R) to uncharged poly(SP-R), while immersed in the DMF:water (3:1) (V:V), the PAH/poly(SP-R) layers would disassemble due to

the diminishing electrostatic interactions between the poly(SP-R) and PAH layers. This process was monitored by UV-Vis spectroscopy. The films were maintained under white light during the test and UV-Vis spectra of the film inside the cuvette (DMF:water (3:1) (V:V)) was recorded in intervals of 30 min and 1 h. The absorbance at $\lambda=345$ nm was chosen and plotted against time to confirm the disassembly progress. The control film was kept in the dark, in the absence of any light irradiation, with measurements performed under the same conditions as for the film disassembly.

Figure 7 documents the absorbance of the (PAH/poly(MC-R))₅ LbL coated glass slide at $\lambda=345$ nm when immersed in DMF: water (3:1) (V:V). Under white light irradiation, the intensity of the absorbance is seen to decrease, eventually reaching a plateau near the baseline (equal to the absorbance of the glass substrate in this solvent system). In contrast, the control film maintained a relatively unchanged absorbance at $\lambda=345$ nm over the same period of time. The almost total disassembly of film occurred over 22 h, as evidenced by an overall decrease of $90.4 \pm 2.9\%$ ($n=2$), relative to the baseline. The first order photo-disassembly constant (k) was estimated by fitting the values of the absorbance at 345 nm using Microsoft Excel Solver and eq. 1 (Figure 8). The photo-disassembly rate constant (k) was found to be $2.69 \times 10^{-3} \text{ min}^{-1}$, with a half-life ($t_{\frac{1}{2}}$) for the disassembly process of 257 min.

Surface profilometry analysis of the film, showed a decrease in height of the (PAH/poly(MC-R))₅ film from ~ 165 nm (Figure S5) to ~ 11 nm after white light irradiation (Figure S7), thereby confirming that disassembly had occurred as suggested by the UV-Vis spectroscopy.

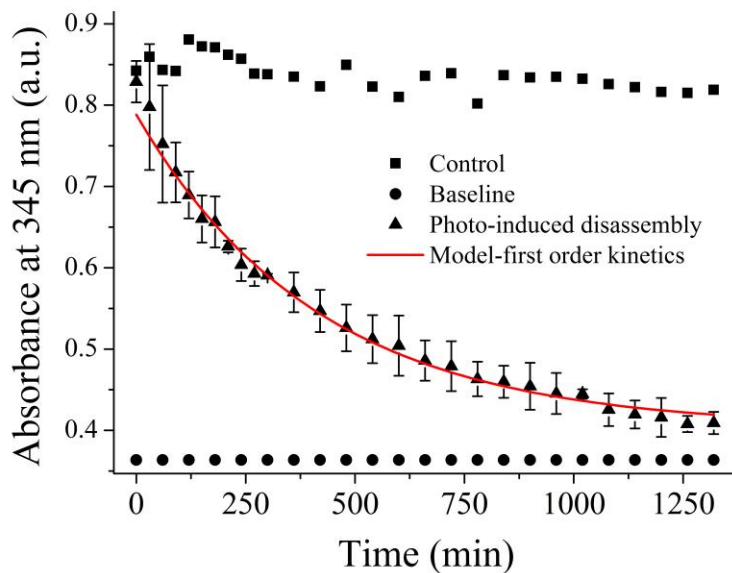


Figure 7. Absorbance at $\lambda=345$ nm of PAH/poly(MC-R)₅ film after white light exposure (blue) and in the dark (black), at different times. The red points represent the absorbance of the glass substrate at 345 nm. The error bars in the blue scatter graph represent the standard deviation of the absorbance at 345 nm for each time interval (n=3).

CONCLUSION

In the work presented herein we have introduced a photochromic linear spiropyran-containing polymer, poly(SP-R), which was polymerized from a monomeric SP-norbornene (SP-R) derivative. The polymer formed LbL films via photo-induced assembly using UV light which could be subsequently disassembled using white light. Solution state UV-Vis measurements of poly(SP-R) showed that the spiropyran photochromism was retained in the polymeric state, thereby confirming that covalent attachment of the spiropyran derivative within the polymer does not adversely affect its reversible switching behaviour.

Via a very simple and efficient method, LbL thin films containing the polymers poly(MC-R) and PAH were created. Successive deposition of up to ten bilayers was achieved, in which the

predominant electronic absorption bands of the MC form was retained, implying the MC form was stabilised by the local charged polymer environment.

The absorbance of the (PAH/poly(MC-R))₅ film was monitored at $\lambda=345$ nm under white light irradiation to follow the disassembly of the film over a 22 h period. The initial thickness of this five-bilayer film was measured using ellipsometry to be ~ 165 nm prior to white light irradiation and ~ 11 nm after, confirming the photo-induced disassembly capacity of film. This study shows that spiropyran-functionalised polymers could be used for the fabrication of stimuli responsive polymeric capsules and formed via layer-by-layer that have the ability to assemble and disassemble using light. This exciting development could be of interest for many potential applications, such as photo-controlled uptake and release of therapeutic agents at precise locations.

SUPPORTING INFORMATION. Layer-by-Layer deposition scheme (Figure 1). ¹H NMR of the linear poly(SP-R) in solution (Figure S2). DLS (Figure S3) and Zeta Potential (Figure S4) of poly(SP-R)/Poly(MC-R) solutions. Surface profilometry of (PAH/poly(MC-R)) LbL films after assembly of five bilayers (Figure S5), first bilayer (Figure S6) and after photo-induced disassembly of the five-bilayer film (Figure S7). This material is available free of charge via the Internet at <http://pubs.acs.org>.

AUTHOR INFORMATION

Corresponding Author

Larisa.Florea@dcu.ie; Tel.: +353-01-700-7699.

ACKNOWLEDGMENTS

The authors acknowledge support from Science Foundation Ireland under the Insight initiative, grant SFI/12/RC/2289, CAPES and CNPq. CD and DD also acknowledge the SFI under the Technology Innovation Development Award no. 16/TIDA/4183. F.B.L. acknowledges the Ramón y Cajal Programme (Ministerio de Economía y Competitividad) and Gobierno de España, Ministerio de Economía y Competitividad, with Grant No. BIO2016-80417-P.

REFERENCES

- (1) Morgan, B.; Dadmun, M. D. The Effect of Illumination on the Depth Profile of Thermally Annealed MEH-PPV/dPS Blends. *J. Polym. Sci. Part B Polym. Phys.* **2017**, *55* (15), 1142–1149.
- (2) Takeuchi, M.; Imai, H.; Oaki, Y. Real-Time Imaging of 2D and 3D Temperature Distribution: Coating of Metal-Ion-Intercalated Organic Layered Composites with Tunable Stimuli-Responsive Properties. *ACS Appl. Mater. Interfaces* **2017**, *9* (19), 16546–16552.
- (3) Nguyen, C. T.; Zhu, Y.; Chen, X.; Sotzing, G. A.; Granados-Focil, S.; Kasi, R. M. Nanostructured Ion Gels from Liquid Crystalline Block Copolymers and Gold Nanoparticles in Ionic Liquids: Manifestation of Mechanical and Electrochemical Properties. *J Mater Chem C* **2015**, *3* (2), 399–408.
- (4) Koçer, G.; ter Schiphorst, J.; Hendrikx, M.; Kassa, H. G.; Leclère, P.; Schenning, A. P. H. J.; Jonkheijm, P. Light-Responsive Hierarchically Structured Liquid Crystal Polymer Networks for Harnessing Cell Adhesion and Migration. *Adv. Mater.* **2017**, *29* (27), 1606407.
- (5) Liu, L.; Zeng, J.; Zhao, X.; Tian, K.; Liu, P. Independent Temperature and pH Dual-Responsive PMAA/PNIPAM Microgels as Drug Delivery System: Effect of Swelling Behavior of the Core and Shell Materials in Fabrication Process. *Colloids Surf. Physicochem. Eng. Asp.* **2017**, *526*, 48–55.
- (6) Iqbal, D.; Samiullah, M. Photo-Responsive Shape-Memory and Shape-Changing Liquid-Crystal Polymer Networks. *Materials* **2013**, *6* (1), 116–142.
- (7) Ma, J.; Xuan, L. Towards Nanoscale Molecular Switch-Based Liquid Crystal Displays. *Displays* **2013**, *34* (4), 293–300.
- (8) Spinks, G. M. Deforming Materials With Light: Photoresponsive Materials Muscle In On the Action. *Angew. Chem. Int. Ed.* **2012**, *51* (10), 2285–2287.
- (9) Niu, D.; Jiang, W.; Liu, H.; Zhao, T.; Lei, B.; Li, Y.; Yin, L.; Shi, Y.; Chen, B.; Lu, B. Reversible Bending Behaviors of Photomechanical Soft Actuators Based on Graphene Nanocomposites. *Sci. Rep.* **2016**, *6* (1).
- (10) Zhao, H.; Hou, B.; Tang, Y.; Hu, W.; Yin, C.; Ji, Y.; Lu, X.; Fan, Q.; Huang, W. O-Nitrobenzyl-Alt-(Phenylethynyl)benzene Copolymer-Based Nanoaggregates with Highly Efficient Two-Photon-Triggered Degradable Properties via a FRET Process. *Polym Chem* **2016**, *7* (18), 3117–3125.

- (11) Irie, M.; Fukaminato, T.; Matsuda, K.; Kobatake, S. Photochromism of Diarylethene Molecules and Crystals: Memories, Switches, and Actuators. *Chem. Rev.* **2014**, *114* (24), 12174–12277.
- (12) Grimm, O.; Wendler, F.; Schacher, F. Micellization of Photo-Responsive Block Copolymers. *Polymers* **2017**, *9* (9), 396.
- (13) Nicoletta, F. P.; Cupelli, D.; Formoso, P.; De Filpo, G.; Colella, V.; Gugliuzza, A. Light Responsive Polymer Membranes: A Review. *Membranes* **2012**, *2* (4), 134–197.
- (14) Johnston, A. P. R.; Cortez, C.; Angelatos, A. S.; Caruso, F. Layer-by-Layer Engineered Capsules and Their Applications. *Curr. Opin. Colloid Interface Sci.* **2006**, *11* (4), 203–209.
- (15) Liang, K.; Such, G. K.; Zhu, Z.; Yan, Y.; Lomas, H.; Caruso, F. Charge-Shifting Click Capsules with Dual-Responsive Cargo Release Mechanisms. *Adv. Mater.* **2011**, *23* (36), H273–H277.
- (16) Delcea, M.; Möhwald, H.; Skirtach, A. G. Stimuli-Responsive LbL Capsules and Nanoshells for Drug Delivery. *Adv. Drug Deliv. Rev.* **2011**, *63* (9), 730–747.
- (17) Achilleos, D. S.; Hatton, T. A.; Vamvakaki, M. Light-Regulated Supramolecular Engineering of Polymeric Nanocapsules. *J. Am. Chem. Soc.* **2012**, *134* (13), 5726–5729.
- (18) Hirshberg, Y. Reversible Formation and Eradication of Colors by Irradiation at Low Temperatures. A Photochemical Memory Model. *J. Am. Chem. Soc.* **1956**, *78* (10), 2304–2312.
- (19) Pennakalathil, J.; Hong, J.-D. Self-Standing Polyelectrolyte Multilayer Films Based on Light-Triggered Disassembly of a Sacrificial Layer. *ACS Nano* **2011**, *5* (11), 9232–9237.
- (20) Thompson, D.; Coleman, S.; Diamond, D.; Byrne, R. Electronic Structure Calculations and Physicochemical Experiments Quantify the Competitive Liquid Ion Association and Probe Stabilisation Effects for Nitrobenzospiropyran in Phosphonium-Based Ionic Liquids. *Phys. Chem. Chem. Phys.* **2011**, *13* (13), 6156.
- (21) Li, Z.; Wan, S.; Shi, W.; Wei, M.; Yin, M.; Yang, W.; Evans, D. G.; Duan, X. A Light-Triggered Switch Based on Spiropyran/Layered Double Hydroxide Ultrathin Films. *J. Phys. Chem. C* **2015**, *119* (13), 7428–7435.
- (22) Keum, S.-R.; Ahn, S.-M.; Roh, S.-J.; Ma, S.-Y. The Synthesis and Spectroscopic Properties of Novel, Photochromic Indolinobenzospiropyran-Based Homopolymers Prepared via Ring-Opening Metathesis Polymerization. *Dyes Pigments* **2010**, *86* (1), 74–80.
- (23) Florea, L.; Hennart, A.; Diamond, D.; Benito-Lopez, F. Synthesis and Characterisation of Spiropyran-Polymer Brushes in Micro-Capillaries: Towards an Integrated Optical Sensor for Continuous Flow Analysis. *Sens. Actuators B Chem.* **2012**, *175*, 92–99.
- (24) Campos, P. P.; Fraceto, L. F.; Ferreira, M. Layer-by-Layer Films Containing Emodin or Emodin Encapsulated in Liposomes for Transdermal Applications. *Colloids Surf. B Biointerfaces* **2018**, *162*, 69–75.
- (25) Dey, T.; Naughton, D. Cleaning and Anti-Reflective (AR) Hydrophobic Coating of Glass Surface: A Review from Materials Science Perspective. *J. Sol-Gel Sci. Technol.* **2016**, *77* (1), 1–27.
- (26) Moniruzzaman, M.; Sabey, C. J.; Fernando, G. F. Photoresponsive Polymers: An Investigation of Their Photoinduced Temperature Changes during Photoviscosity Measurements. *Polymer* **2007**, *48* (1), 255–263.
- (27) Florea, L.; McKeon, A.; Diamond, D.; Benito-Lopez, F. Spiropyran Polymeric Microcapillary Coatings for Photodetection of Solvent Polarity. *Langmuir* **2013**, *29* (8), 2790–2797.

- (28) Abdollahi, A.; Alinejad, Z.; Mahdavian, A. R. Facile and Fast Photosensing of Polarity by Stimuli-Responsive Materials Based on Spiropyran for Reusable Sensors: A Physico-Chemical Study on the Interactions. *J Mater Chem C* **2017**, *5* (26), 6588–6600.
- (29) Abdollahi, A.; Rad, J. K.; Mahdavian, A. R. Stimuli-Responsive Cellulose Modified by Epoxy-Functionalized Polymer Nanoparticles with Photochromic and Solvatochromic Properties. *Carbohydr. Polym.* **2016**, *150*, 131–138.
- (30) De Barros, A.; Constantino, C. J. L.; Bortoleto, J. R. R.; Da Cruz, N. C.; Ferreira, M. Incorporation of Gold Nanoparticles into Langmuir-Blodgett Films of Polyaniline and Montmorillonite for Enhanced Detection of Metallic Ions. *Sens. Actuators B Chem.* **2016**, *236*, 408–417.
- (31) Makiura, R.; Motoyama, S.; Umemura, Y.; Yamanaka, H.; Sakata, O.; Kitagawa, H. Surface Nano-Architecture of a Metal–organic Framework. *Nat. Mater.* **2010**, *9* (7), 565–571.
- (32) Goulet, P. J. G.; dos Santos, D. S.; Alvarez-Puebla, R. A.; Oliveira, O. N.; Aroca, R. F. Surface-Enhanced Raman Scattering on Dendrimer/Metallic Nanoparticle Layer-by-Layer Film Substrates. *Langmuir* **2005**, *21* (12), 5576–5581.
- (33) dos Santos, Jr., D. S.; Aroca, R. F. Selective Surface-Enhanced Fluorescence and Dye Aggregation with Layer-by-Layer Film Substrates. *The Analyst* **2007**, *132* (5), 450.
- (34) Lin, Y.; Ma, L.; Li, Y.; Liu, Y.; Zhu, D.; Zhan, X. Small-Molecule Solar Cells with Fill Factors up to 0.75 via a Layer-by-Layer Solution Process. *Adv. Energy Mater.* **2014**, *4* (1), 1300626.
- (35) Llamas, S.; Guzmán, E.; Ortega, F.; Baghdadli, N.; Cazeneuve, C.; Rubio, R. G.; Luengo, G. S. Adsorption of Polyelectrolytes and Polyelectrolytes-Surfactant Mixtures at Surfaces: A Physico-Chemical Approach to a Cosmetic Challenge. *Adv. Colloid Interface Sci.* **2015**, *222*, 461–487.
- (36) Jiang, C.; Liu, X.; Luo, C.; Zhang, Y.; Shao, L.; Shi, F. Controlled Exponential Growth in Layer-by-Layer Multilayers Using High Gravity Fields. *J. Mater. Chem. A* **2014**, *2* (34), 14048.
- (37) Elosua, C.; Lopez-Torres, D.; Hernaez, M.; Matias, I. R.; Arregui, F. J. Comparative Study of Layer-by-Layer Deposition Techniques for Poly(sodium Phosphate) and Poly(allylamine Hydrochloride). *Nanoscale Res. Lett.* **2013**, *8* (1), 539.
- (38) Spera, M. B. M.; Taketa, T. B.; Beppu, M. M. Roughness Dynamic in Surface Growth: Layer-by-Layer Thin Films of Carboxymethyl Cellulose/Chitosan for Biomedical Applications. *Biointerphases* **2017**, *12* (4), 04E401.
- (39) Han, T.-H.; Lee, E.-S.; Ko, T.-H.; Seo, M.-K.; Kim, H.-Y.; Kim, H. J.; Kim, B.-S. Hierarchically Assembled Nanofibers Created by a Layer-by-Layer Self-Assembly. *J. Nanosci. Nanotechnol.* **2016**, *16* (4), 4080–4085.

Graphical Abstract:

